

## SOLAR-CYCLE VARIATIONS OF INTERNETWORK MAGNETIC FIELDS

M. Faurobert<sup>1</sup> and G. Ricort<sup>1</sup>

**Abstract.** Small-scale magnetic fields in the quiet Sun contain in total more flux than active regions and represent an important reservoir of magnetic energy. But the origin and evolution of these fields still remain largely unknown. We present a study of the solar-cycle and center-to-limb variations of the magnetic-flux structures at small scales in the solar internetwork. We used Hinode SOT/Spectropolarimetric data from the irradiance program from 2008 to 2016 and applied a deconvolution to the intensity and polarization profiles to correct them from the smearing due the Point Spread Function of the telescope. Then we performed a Fourier spectral analysis of the spatial fluctuations of the magnetic-flux density in  $10'' \times 10''$  internetwork regions spanning a wide range of latitudes. At low and mid latitudes and away from the active latitudes present at solar maximum, the power spectra do not vary significantly with the solar cycle. At high latitudes variations in opposition of phase with the solar cycle are observed at granular scales. Whatever the latitude the power of the magnetic fluctuations at scales smaller than  $0.5''$  remain constant throughout the solar cycle. These results are in favor of a small-scale dynamo that operates in the internetwork.

Keywords: solar magnetism, high resolution, solar cycle

### 1 Introduction

The internetwork (IN) refers to the regions of the solar surface that are outside of active regions and the magnetic network. It has been shown that IN magnetic fields bring large amounts of magnetic flux at small scales to the solar surface and may play an important role in the heating of the chromosphere. A very thorough review of the numerous and sometimes contradictory observational investigations of the quiet Sun magnetism is presented in Bellot Rubio & Orozco Suárez (2019). Many high resolution spectro-polarimetric observations have shown that IN magnetic fields emerge at the solar surface on the form of magnetic loops with various sizes and lifetimes. State-of-heart simulations show that magnetic loops are a consequence of the interaction of convective flows with the magnetic field.

However, as noted in Bellot Rubio & Orozco Suárez (2019), the origin of IN magnetic fields is still debated. Are they due to the recycling of decaying active regions or generated by the solar dynamo in the deep convection zone? Alternatively they may be produced by a local dynamo operating at the solar surface. In this paper we address this issue by investigating the spatial structuring of IN magnetic flux and whether it varies according to the latitude and the global solar cycle. Using synoptic data from the Hinode irradiance program between 2008 and 2016, we obtain maps of the longitudinal magnetic flux density on a wide range of latitudes. We correct these maps from the smoothing effect of the Point Spread Function (PSF) of the telescope and from a time-varying defocus, then we select a set of 162 ( $10'' \times 10''$ ) IN regions between the equator and  $\pm 70^\circ$ . We perform a Fourier analysis of the unsigned magnetic-flux spatial fluctuations in these regions and examine the solar-cycle variations of their Fourier power spectra at various latitudes,

### 2 Principal component analysis of the Stokes profiles and deconvolution

Following Quintero Noda et al. (2015) we work on the spectral dimension of the Stokes parameters and not on the spatial dimensions. We write the Stokes profiles at each pixel as a linear combination of an orthonormal

---

<sup>1</sup> University Cote d'Azur, Lagrange Laboratory. Parc Valrose. 06108 Nice Cedex 2. France

basis of eigenfunctions  $\Phi_i(\lambda)$  that are obtained through a principal component analysis of the observed profiles  $S_p(\lambda, x, y)$ ,

$$S_p(\lambda, x, y) = \sum_{i=1}^{n_\lambda} (\omega_i(x, y) * PSF(x, y)) \Phi_i(\lambda) + N(x, y), \quad (2.1)$$

where the star operator denotes the convolution and  $N(x, y)$  is some additive noise. The scalar product of the observed Stokes profiles with any of the eigenfunctions gives

$$\langle S_p(\lambda, x, y), \Phi_k(\lambda) \rangle = \omega_k(x, y) * PSF(x, y) + N(x, y). \quad (2.2)$$

Therefore the maps of the coefficients of the linear combination obtained from the observed Stokes profiles are affected by the same convolution with the PSF as the profiles. We recover the coefficients  $\omega_k$  by applying a PSF deconvolution to the observed  $\omega_k$ -maps, and we reconstruct the Stokes profiles using the linear combination of the eigenfunctions with the  $\omega_k$  coefficients. We find that 8 principal components are sufficient to account for the variability of the observed profiles. The method also allows an efficient filtering of the noise that is mainly projected on less significant principal components.

For our long-term study we chose to deal with the Stokes I and V profiles only, linear polarization profiles in the irradiance data of Hinode are much more noisy and their quality is degrading after 2013. We do not use any sophisticated inversion method to recover the magnetic field components from the Stokes profiles but rather implement the simple and robust center-of-gravity method, which was first introduced by Semel (1970) and later extensively tested by Uitenbroek (2003) by comparison with the magnetic flux in 3D magnetohydrodynamical simulations of the magneto-convection in the solar photosphere.

In the center-of-gravity method the line-of-sight component of the magnetic field is derived from the wavelengths  $\lambda_+$  and  $\lambda_-$  of the centroid of the right- and left-circularly polarized line components  $I \pm V$ ,

$$\lambda_{\pm} = \frac{\int \lambda (I_{cont} - (I \pm V)) d\lambda}{\int (I_{cont} - (I \pm V)) d\lambda}, \quad (2.3)$$

where  $I_{cont}$  denotes the continuum intensity. The longitudinal magnetic component is then obtained from the relation

$$B_{LOS} = \frac{\lambda_+ - \lambda_-}{2} \frac{4\pi mc}{e g_L \lambda_0^2}, \quad (2.4)$$

where  $g_L$  is the line effective Landé factor and  $m$  and  $e$  are the mass and electric charge of the electron (in MKSA units), respectively. When the magnetic structure is not resolved by the instrument, Eq. (2.4) gives the longitudinal apparent flux density, that is, the magnetic flux density averaged over the pixel area. We remark that because the wavelengths  $\lambda_{\pm}$  are obtained from a ratio of observed intensities, they should not be greatly affected by a possible aging of the detectors or calibration issues. Figure 1 shows the magnetic flux map of an IN region at disk-center in 2014 before and after deconvolution. The sharpening effect of the deconvolution leads to higher flux densities in the corrected map.

### 3 Fourier power spectra of the magnetic flux density

We use one run of the irradiance program HOP79 per year from 2008 to 2016. For each year we have selected 162 IN regions of  $10'' \times 10''$  located along the polar axis from the north to the south pole. The original pixel size of the data is  $0.1475'' \times 0.32''$ , we performed bilinear interpolations of the images to get a square pixel of  $0.16''$  that is the size of the camera pixel. Figure 2 shows the mean unsigned magnetic flux in the selected regions in 2008 (solar minimum) and in 2014 (solar maximum). We observe no significant latitudinal variation nor variation between the solar minimum and maximum, except at some active latitudes in 2014.

We computed the 2D Fourier spectra of the IN unsigned flux density after dividing each selected region in four subregions of  $32 \text{ px} \times 32 \text{ px}$  ( $5'' \times 5''$ ), we then further averaged the spectra over 9 IN regions at close latitudes. We then obtain 18 power spectra spanning latitudes between  $\pm 70^\circ$ . Out of disk-center the radial averages of the 2D spectra are computed over elliptical bands instead of circular bands to account for the shortening of the images in the radial direction due to the projection effect. As the mean value of the unsigned flux density varies very little with the latitude and time we show spectra normalized by the mean unsigned flux density in the regions.

Figure 3 shows the normalized power spectra at disk-center and at high latitudes in 2008, 2009, 2013 and 2014 together with the one-sigma bars computed on the 9 regions used for the averaging. We observe no significant

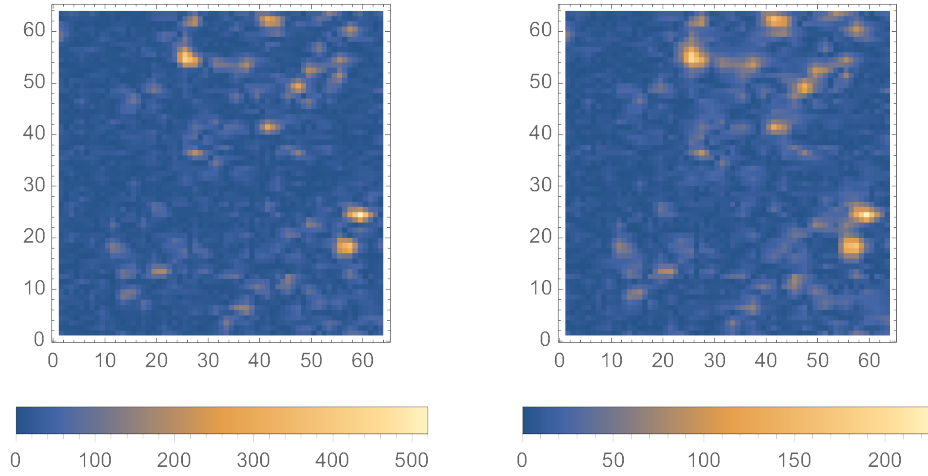


**Fig. 1.** Maps of the unsigned longitudinal magnetic flux density in a selected IN region. The axis are in pixels of  $0.16''$ . Left: after deconvolution, right: before deconvolution.

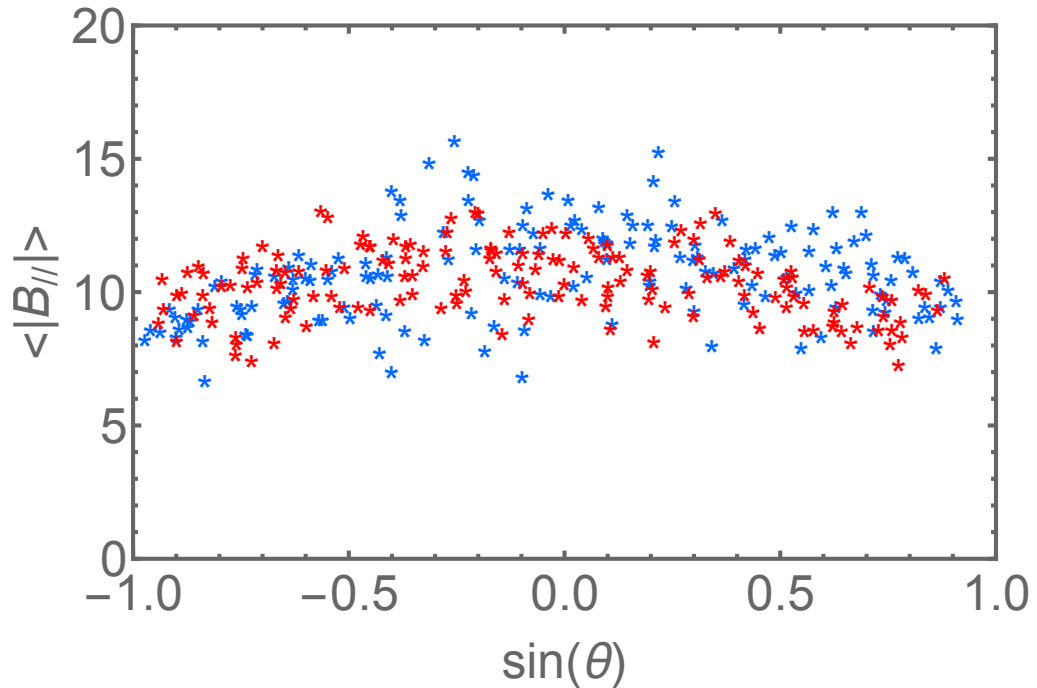


**Fig. 2.** Mean unsigned magnetic flux density in  $\text{Mx}/\text{cm}^2$  in the selected IN regions in 2008 (red symbols) and in 2014 (blue symbols) as a function of the sinus of their latitude.

variation of the power spectra at disk-center but at high latitudes the power at low spatial frequencies (scales between  $5''$  and  $0.5''$ ) decreases significantly at the maximum of the solar cycle. We observed that the minimum of the cycle takes places in 2009 at the North pole, and in 2008 at the South pole. We observe no variation at spatial frequencies larger than  $2 \text{ arcsec}^{-1}$  (scales smaller than  $0.5''$ ), this is also true at all the latitudes of our data sets.

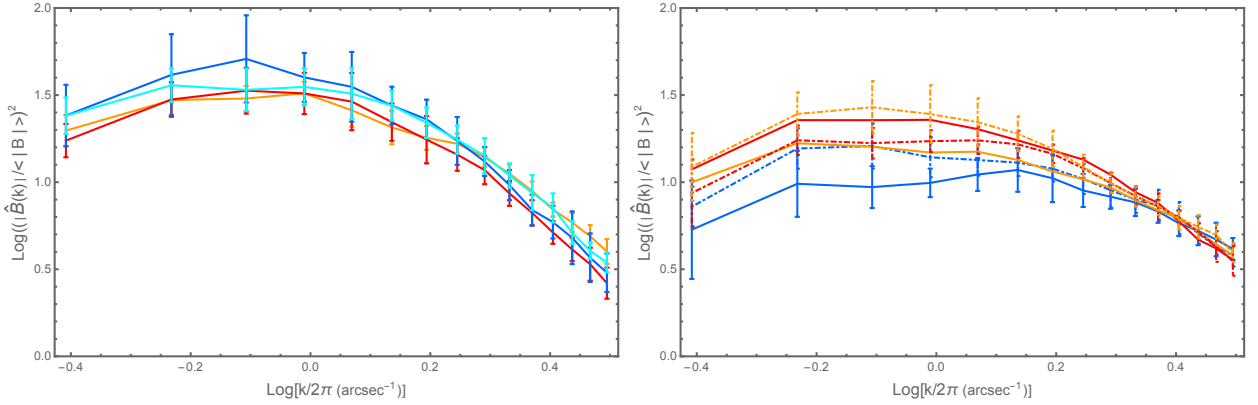


**Fig. 3. Left:** Normalized power spectra at disk-center in 2008 (red curve), 2009 (orange), 2013 (light blue), 2014 (blue). **Right:** Normalized power spectra at high latitudes. Full lines:  $-70^\circ$ , dot-dashed curves:  $+70^\circ$ . In 2008 (red), 2009 (orange), 2014 (blue). The bars show one standard deviation computed on 9 IN regions at close latitudes.

#### 4 Conclusions

We recall that the longitudinal flux reflects different magnetic components at disk center and high latitudes. At disk center the line of sight is vertical so we observe vertical fields, whereas at high latitudes it is inclined on the solar surface so we observe mainly the horizontal fields of the selected IN regions. As the heliocentric angle is larger at high latitude we also observe higher layers of the photosphere. It has been shown that magnetic fields in the IN have a more uniform distribution of field inclinations than network and other strong-field regions and that the inclination increases with height.

Our study shows that vertical fields in the IN at low latitudes do not vary significantly with the solar cycle, at least on the spatial scale that we could investigate, between  $0.3''$  and  $5''$ . The horizontal fields observed at high latitudes show variations in opposition of phase with the solar cycle, except at scales smaller than  $0.5''$ , where the power spectra remain constant.

At scales smaller than  $0.5''$  the power spectra of the IN longitudinal magnetic flux density are constant whatever the latitude, indicating the presence of a time-independent magnetic component. The time-independence of the spectra is a strong indication that the mechanism at the origin of IN fields is not, at least not directly, correlated to the global dynamo.

It is difficult to compare our observational results with the numerical simulations of Rempel (2014, 2018) because we measured the unsigned longitudinal flux and not the magnetic energy. In the simulations the magnetic energy power spectrum at disk-center has a broad maximum at small spatial scales on the order of 500 km to 1000 km. In our data, the power spectra have a broad maximum at sub-granular spatial scales on the order of 900 km, this is consistent with the simulations.

#### References

- Bellot Rubio, L. & Orozco Suárez, D. 2019, *Living Reviews in Solar Physics*, 16, 1  
 Quintero Noda, C., Asensio Ramos, A., Orozco Suárez, D., & Ruiz Cobo, B. 2015, *A&A*, 579, A3  
 Rempel, M. 2014, *ApJ*, 789, 132  
 Rempel, M. 2018, *ApJ*, 859, 161  
 Semel, M. 1970, *A&A*, 5, 330  
 Uitenbroek, H. 2003, *ApJ*, 592, 1225